HW 1

Topocentric Coordinates, Angles-Only IOD, Minimum Energy and Lambert's Solution

Justin Self

AERO557: Advanced Orbital Mechanics

February 1, 2024

Problem 1

Topocentric Coordinates.

HST TLEs:

```
1 20580U 90037B 24010.28323428 .00005912 00000-0 29430-3 0 9991
2 20580 28.4707 327.8603 0002613 104.9653 10.4281 15.15476605652889
```

Predict the look angles (RA/DEC and Az/El) and associated times for SLO (coordinates listed below) on Jan 11.
Here are the look angles from Heaven's Above:

```
Date Mag time. El Az. Time. El. Az. Time. El Az. Pass type
11 Jan 2.0 18:50:29 10° SW 18:53:58 28° S 18:54:32 27° SSE visible
```

Discuss the differences.

SLO Coordinates: 35.3540 north 120.3757 west 105.8 m altitude

Solution.

See Appendix A for results and code for Problem 1

Given initial Two Line Elements (TLEs) for the Hubble Space Telescope (HST), look angles were calculated using a blend of homemade, AERO557 provided, publicly published, and native `MATLAB` code. Since the problem statement asked for look angles and times for *January 11*, the simulation was modelled to consider visible HST passes between 11 Jan 2024 00:00:00 (local time) to 11 Jan 2024 23:59:59 (local time). Consequently, the HST orbit was propagated from the epoch date (10 January 2024 06:47:51, UTC) to the mission start date (11 Jan 08:00:00, UTC).

The initial orbit propagation method was a two-body motion propagator using the `MATLAB ODE45` ODE solver. Orbital perturbations were *not* simulated as a condition of the problem given, which very likely led to errors in look angle predictions, specifically with respect to time and elevation. Fig. 1 shows the osculating orbit propagated from the TLE retrieval epoch to mission start time and positions of the HST at each time.

Once the orbit was propagated to the mission start time (00:00:00 Jan 11, site time) using the two-body propagator, the simulation then used a universal variable propagator at one-second time intervals. Fig. 2 shows a graphical representation of conditions needed for viewing the HST on pass visible from SLO. THe conditions are:

- The spacecraft must be illuminated by the sun
- The site must be in darkness
- Spacecraft must be above the horizon ($180^\circ \leq el \leq 0^\circ$)

The first two conditions are plotted against mission time in Fig. 2, with two candidate time blocks highlighted in black.

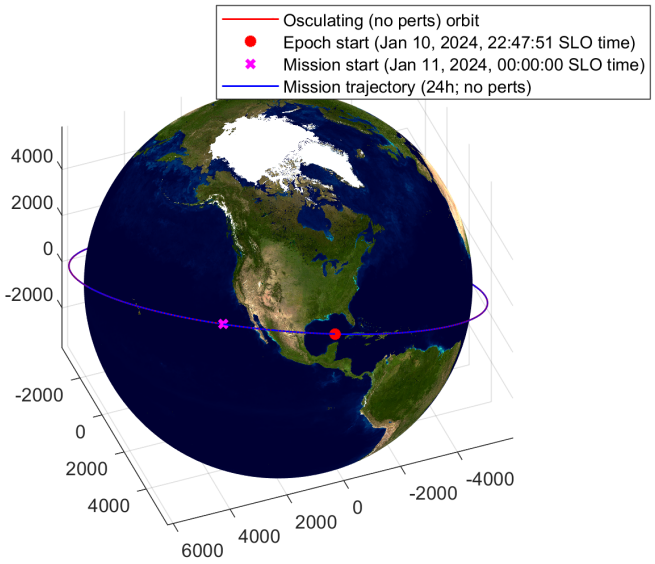

Figure 1: Osculating orbit trajectory (ECI) of HST starting at epoch (TLE retrieval) and mission start time (00:00:00 11 Jan, 2024; Pacific Standard Time). HST was propagated until 11 Jan 23:59:59 without perturbations, which led to small errors in elevation, azimuth, and viewing times. Planet3D visualization code courtesy of Tamas Kis, throughout.

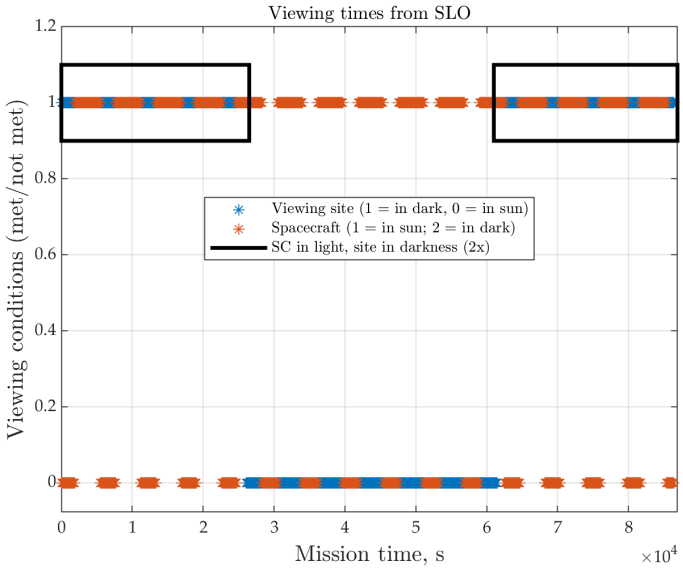

Figure 2: Graphic representation of viewing conditions from SLO, California. Zero means the spacecraft is either in eclipse or the site is in daylight. One means the spacecraft is in the sun or the site is in darkness. No masking is applied, so any viewing elevation > 0 will be captured. The black boxes highlight HST viewing candidate regions.

After propagating the orbit and computing changing conditions at each time step, the data was filtered the third condition (spacecraft must be between 0° and 180°). Fig. 3 shows the elevation and associated times of HST flybys from the local SLO frame. Note that there

are three candidate flybys on 11 Jan 2024:

a) 17:11 - 17:21 max el: 10.3°

b) 18:50 - 18:57, max el: 23.8°

c) 20:31 - 20:32, (no max elevation reached)

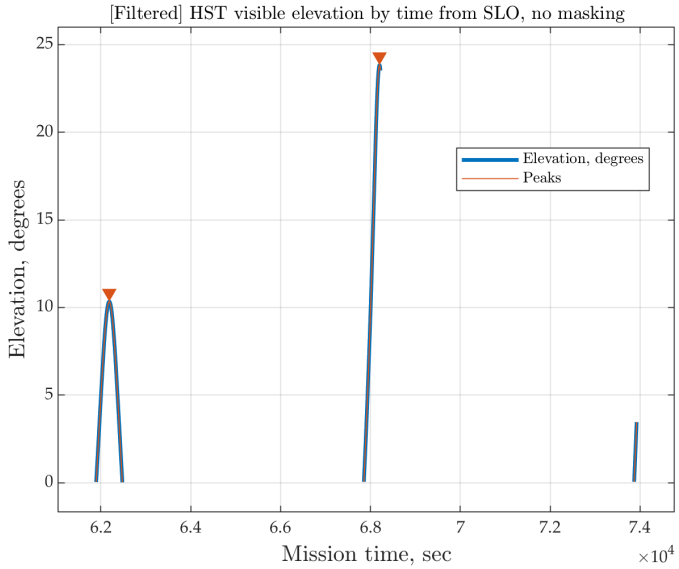

Figure 3: Elevation peaks and associated times for HST viewing from SLO on 11 Jan, 2024. This plot comes from the right-hand side block highlighted in Fig. 3. This means the only visible passes of HST from the site between 11 Jan (00:00:00 local) and 12 Jan (23:59:59 local) occurred at these times.

Of the three candidates, the second view corresponds closely with the data given by Heavens-Above (see Fig. 4). Notably, Heavens-Above applies a 10° mask to their view angle calculations, and ours does not. Thus, View 3 would not show up on H-A datasets. It is likely that this is why View 1 (max elevation ~ 10°) doesn't show up on H-A.

The reason our viewing times are off could be due to several reasons. First, orbital perturbations were not considered in this simulation. Over a time span of 24 hours, the COEs would have changed due to zonal harmonics, solar radiation pressure, n-body effects, and atmospheric drag. Secondly, HST could also have performed a thrust maneuver during the time span after initial TLE retrieval. Thirdly, H-A doesn't start recording a pass until the sun is 6° below the horizon (both rising and setting)[1]:

```
We have a cut-off of -6° sun altitude for our predictions, so that
satellite passes are only predicted when the sky is reasonably dark.
However, these bright satellites can sometimes be seen when the
sun is higher, but this explains why they aren't in the list.
```

Fourthly, our model does not apply the same 10° masking that H-A does. This would skew the viewing times. These are all plausible reasons why our simulation does not match

exactly with the H-A predictions. Figs. 5, 6, 7, and 8 show our simulation results, which agree reasonably with H-A predictions given in Fig. 4.

Date	Mag	time.	El	Az.	Time.	El.	Az.	Time.	El	Az.	Pass type
11 Jan	2.0	18:50:29	10°	SW	18:53:58	28°	S	18:54:32	27°	SSE	visible

Figure 4: Given viewing times/angles for HST from Heavens-Above. Note that the Heavens-Above HST pass algorithm appears to build in a 10° elevation mask, so published passes begin at 10°.

	View 1	View 2	View 3
Start	11-Jan-2024 17:11:35	11-Jan-2024 18:50:53	11-Jan-2024 20:31:08
Peak	11-Jan-2024 17:16:26	11-Jan-2024 18:56:41	11-Jan-2024 20:32:04
Stop	11-Jan-2024 17:21:18	11-Jan-2024 18:57:02	11-Jan-2024 20:32:04

Figure 5: Of the three visible passes, View 2 matches Heavens-Above data shown in Fig. 4. This is likely due to the 10° elevation mask, which would remove View 1 and View 3. The times are similar, but not exact. This is likely due to perturbational effects, not considered in this model.

	View 1	View 2	View 3
Start az [deg]	208.661795516048	236.701274199645	253.922750831431
Peak az [deg]	157.092014219895	168.413783014575	250.947287773236
Stop az [deg]	105.596469629532	159.966604786374	250.947287773236

Figure 6: Azimuths for three calculated HST viewing times from SLO between 11 Jan and 12 Jan, 2024.

	View 1	View 2	View 3
Start az direction	{'SSW'}	{'SW' }	{'WSW'}
Peak az direction	{'SSE'}	{'S' }	{'WSW'}
Stop az direction	{'ESE'}	{'SSE'}	{'WSW'}

Figure 7: Compass directions for three calculated HST viewing times from SLO between 11 Jan and 12 Jan, 2024. Note that View 2 agrees with the H-A data given in Fig. 4.

	View 1	View 2	View 3
Start el [deg]	0.0359222620314736	0.0456622012614463	0.0480099784863766
Peak el [deg]	10.3357511324859	23.8335804788815	3.45902152009376
Stop el [deg]	0.0178591802397283	23.5284460587052	3.45902152009376

Figure 8: Predicted elevation for visible HST passes as seen from SLO from 11 Jan to 12 Jan, 2024. Note that our predictions do not include elevation masking, as H-A does (see Fig. 4). Max elevations are also slightly off, likely due to perturbational effects (not considered in this model).

Problem 2

Gauss, Extended Gauss, and Double-R methods for angles-only initial orbit determination.

Calculate the position and velocity vectors from the double-r method and Gauss' method (non-extended and extended) for topocentric angles only observations.

In addition, compare the resulting COEs from the state vectors as well. Discuss the differences and thoughts on each of the methods. Please note, in the future, the Gauss method is always run with the extension. Finally, pick what TLE object might be close for this object (assume no perturbations) and just compare the COES.

```
Observation RA (degs) DEC (degs) Date (UT) Time (UT)
1 30.381 23.525 03-25-2013 03:10:30.032
2 65.134 0.774 03-25-2013 03:15:20.612
3 99.976 -30.44 03-25-2013 03:20:32.777
```

Observations are taken at Cal Poly Observatory:
35.30 north, 120.66 west, 105.8 m altitude

```
TLE options:
1 25623U 99004C 13109.04882318 -.00000094 00000-0 -16690-3 0 1204
2 25623 051.9974 067.7982 0012092 184.1231 215.4516 11.86494224651645

1 25165U 98008D 13083.14572197 -.00000211 00000-0 -12941-2 0 4434
2 25165 052.0160 303.6990 0005433 319.9573 182.6276 12.12023409691559

1 25946U 99058D 13104.16396495 -.00000071 00000-0 19175-3 0 939
2 25946 051.9981 329.5396 0000986 149.5293 353.4996 12.46940793622716
```

Solution.

See Appendix B for results and code for Problem 2

Position and velocity vectors for the middle of three observations were determined using a home-built function called `gauss.m` allowing users to choose between Gauss and Gauss

Extended methods. These methods were compared with the Double-R angles-only method. Tabulated results are shown in Fig. 9. Fig. 10 gives the associated Common Orbital Elements (COEs) from each method.

Gauss' technique using angles-only data is said to work best when the angular separation between observations is less than 60°, but it is shown to perform remarkably well for data separated by 10° or less [2]. In this analysis, the Gauss method (not extended) produced the least accurate (when compared to the Double-R method) results of the three methods utilized. Both Gauss and Gauss extended models utilized the Gibbs initial orbit determination algorithm before iterative processing (if using extended).

The Double r-iteration method is a combination of numerical and dynamical techniques proposed by Escobal (1965) and is more robust than the Gauss method. This method, according to [2], can handle observations that are days apart. This method still utilizes the familiar t_m (transfer method) variable (+1) for the short way, (−1) for the long way (retrograde) transfer trajectory. The initial guess is important in this method. In our case, this method produced the most accurate results, shown in Figs. 9 - 10.

	Gauss	Gauss Extended	Double-R
r2x [km]	-840.054378084647	-823.006650676095	-823.007283505782
r2y [km]	7070.6739188924	7107.45724373507	7107.45587829911
r2z [km]	3698.23881177458	3698.78651819708	3698.78649786563
v2x [km/s]	-5.28758213855778	-5.29401099273387	-5.29400816978208
v2y [km/s]	1.79781989089623	1.80435321941347	1.80435266589727
v2z [km/s]	-4.64317551818809	-4.65391220082394	-4.65390969069674

Figure 9: Position and velocity vectors obtained from three IOD angles-only methods.

	Gauss	Gauss Extended	Double-R
h [km2/s]	58274.1435320561	58604.7693607567	58604.7304178864
inc [deg]	52.0008016878705	51.9239527750232	51.9239576964323
RAAN [deg]	300.715297695514	300.495990828433	300.495997043193
ecc	0.0618157954365597	0.0697770403678169	0.0697757707427007
omega [deg]	144.505649267153	144.798820240989	144.798765881347
True anomaly [deg]	359.697400920804	359.513483519477	359.513535001091
Semi-major axis [km]	8552.18734293876	8658.61243071461	8658.59938178775
Period [s]	7870.94776097365	8018.32531132595	8018.30718535567

Figure 10: COEs obtained from the state vectors obtained by the three IOD angles-only methods.

After computing state vectors and COEs from each method, the next step is to compare the given TLEs with the calculated ones. Relative errors (absolute value of the differences) were plotted and a heatmap generated to compare the two datasets, using the Double-R method as the calculation of choice (see Fig. 11. At first glance, it appears that C is the winner, since there is less error overall. However, it is important to note that all three *inclinations* (A, B, C) are very close to the calculated values. Thus, it is expected that RAAN will be close also. It is clear from Figs. 11 and 12 that both inclination and RAAN agree

reasonably. The eccentricity calculation, although verified against the three IOD methods, did not agree with any of the TLE data. However, all calculation methods and given TLEs give eccentricities near zero.

Since the calculated orbit is very close to circular, any error in argument of perigee may be ignored since ω is inaccurate for highly circular orbits. Furthermore, a is calculated using apogee and perigee radii, and thus a circular orbit will further confound any semi major axis calculations. Period is nearly the same. Revs per day are very close. Thus, TLE B seems to be the correct TLE.

	A	B	C
Err: inc [deg]	0.0734423035677025	0.0920423035677018	0.0741423035677045
Err: RAAN [deg]	232.697797043193	3.2030029568067	29.0436029568067
Err: ecc	0.0685665707427007	0.0692324707427007	0.0696771707427007
Err: omega [deg]	39.3243341186534	175.158534118653	4.73053411865337
Err: n-bar [rev/day]	7.92379852949584e-05	7.92379852949584e-05	0.00012319597073595 6
Err: Semi-major axis [km]	538.563868872739	538.563868872739	803.148351942793
Err: Period [h]	0.204541699405458	0.204541699405458	0.30259708129297

Figure 11: Difference (error) calculations between the provided TLEs and the calculated TLEs based on the Double-R method with colorscale for heatmap error (green for low error, orange and red for high error values).

	TLE B: 25165	Double-R
inc [deg]	52.016	51.9239576964323
RAAN [deg]	303.699	300.495997043193
ecc	0.0005433	0.0697757707427007
omega [deg]	319.9573	144.798765881347
n-bar [rev/day]	12.12023409	10.775341727715
Semi-major axis [km]	8120.03551291501	8658.59938178775
Period [h]	2.02276585208223	2.22730755148769

Figure 12: Comparison between the Double-r iteration calculation and the most likely TLE candidate. Note that inc and RAAN are very close, as is expected. Eccentricity is off, but both are very circular. Semi major axis and argument of perigee values are off, but not surprisingly, due to the circularity of the orbit.

Problem 3

Lambert's Problem Solutions Comparison.
Using universal variable method, Gauss' method, Izzo/Gooding method, and minimum energy, find and compare the velocity vectors for the orbit give two positions, a difference in time, and going the short way around. Please compare the COES as well as the vectors. Discuss why the answers vary.

```
r0 vect = 15,945.34 (Ihat)(km)
r1 vect = 12,214.83899 (Ihat) +  10,249.46731 (Jhat)(km)
tm = short way
deltat = 76.0 mins
```

Solution.

See Appendix C for results and code for Problem 3

Four methods for solving Lambert's problem were employed for the initial orbit determination for two position vectors (given in ECI) and a time between the two observations. No simplifying assumptions were made, since these vectors lie in a plane (no z term). The universal variable, Gauss, and minimum energy algorithms were a blend of homemade and AERO557-provided functions, while the Izzo-Gooding function was retrieved from `MATLAB` Central. All calculations were validated against Vallado's Example 7.5 (third edition). Results are shown in Figs. 13 - 16.

Why the differences?

As in Problem 2, the Gauss method is useful when angular separation is less than 10°, and especially when the extended mode is used. The initial position vectors have an angular separation of $\Delta\nu = 40°$. This is one reason why the Gauss method is not as accurate as the other methods.

The Universal Variable and Izzo-Gooding methods performed nearly identically; at least to the third decimal (sometimes the fourth) in velocities and very close in the COEs. According to [2], numerical analysis indicates that the universal-variable and Battin approaches [not studied here] provide the most accurate answer. The Izzo-Gooding method, a relatively new method, claims robustness and accuracy with two algorithms in one code. In this study we assumed a zero-rev solution; both position vectors were obtained in a single pass.

Finally, the minimum energy approach was used to determine not only the velocity vectors (using a Lambert's solver inside the function after computing the minimum energy state), but also the *minimum energy* semi major axis and minimum energy transfer time, Δt_m, between the two position vectors. This minimum energy transfer time was compared with the parabolic solution (non-elliptical) and the transfer time is given in Figs. 15 and 16. Note that the minimum energy transfer time is slightly lower (75.67 minutes) than the given transfer time (76 minutes); this is a coincidence.

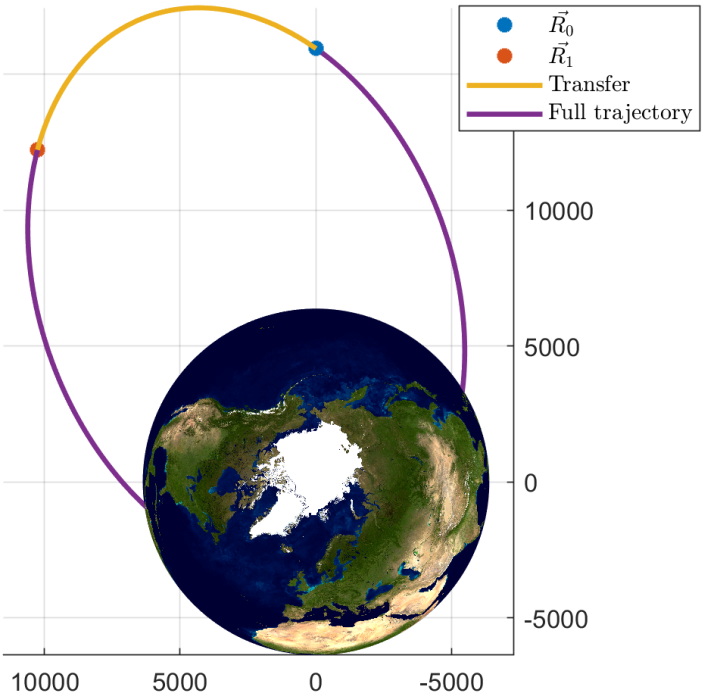

Figure 13: Solution to Lambert's problem for the two given position vectors. Since the trajectory crashes into earth, any number of speculative ideas may be made about the origin and nature of the observed object. This trajectory is confirmed using the four IOD methods and is validated against the example in [2].

```
*** Gauss Method
V0 (Gauss Method) is: 3.5705 km/s
V1 (Gauss Method) is: 3.5705 km/s

*** Universal Variable Method
V0 (Universal Variable Method) is: 3.5696 km/s
V1 (Universal Variable Method) is: 3.5696 km/s

*** Izzo-Gooding Method
V0 (Izzo-Gooding Method) is: 3.5696 km/s
V1 (Izzo-Gooding Method) is: 3.5696 km/s
*** Minimum Energy Method
V0 (Minimum Energy Method) is: 3.5695 km/s
V1 (Minimum Energy Method) is: 3.5695 km/s
```

Figure 14: Speeds obtained from the four IOD methods explored

Finally, the COEs were compared. All methods agreed fairly reasonalby (Gauss being the worst), and all gave 0° inclinations and unsolvable RAAN and argument of perigee values. For an equatorial planar orbit, Ω and ω are indeed unsolvable, since no node line exists between two parallel planes.

	Gauss Method	Universal Variable	Izzo-Gooding Method	Minimum Energy Method
v0x [km/s]	2.05994333876808	2.05888373419334	2.05891074466021	2.04738185098226
v0y [km/s]	2.91633934210809	2.91598259490204	2.91596375936091	2.92401986811616
v0z [km/s]	0	0	0	0
Trajectory Time, h	76	76	76	75.6708777398771
v1x [km/s]	-3.4525924722187	-3.45155388135579	-3.45156246532114	-3.44790918737414
v1y [km/s]	0.909941481474434	0.910347262312584	0.910315471457215	0.923897438948356
v1z [km/s]	0	0	0	0

Figure 15: Velocity vectors associated with the two known position vectors obtained from four IOD methods

	Gauss Method	Universal Variable	Izzo-Gooding Method	Minimum Energy Method
h [km2/s]	46502.0223652899	46496.3339097953	46496.0335706879	46624.4909638674
inc [deg]	0	0	0	0
raan [deg]	NaN	NaN	NaN	NaN
ecc	0.702175159721244	0.702201150091742	0.702205826390994	0.700202980087835
w [deg]	NaN	NaN	NaN	NaN
a [km]	10701.4153631316	10699.5677438606	10699.5681389674	10699.4838536717

Figure 16: COEs obtained from the four IOD methods

References

[1] Chris Peat. *Frequently Asked Questions*. Heavens-Above, 2024.

[2] David A Vallado. *Fundamentals of astrodynamics and applications*, volume 12. Springer Science & Business Media, 2001.